PERGAMON

International Journal of Heat and Mass Transfer 42 (1999) 821–832

International Journal of HEAT and MASS TRANSFER

Experimental study of double-diffusive convection in a rotating annulus with lateral heating

Jinho Lee[a,*], Shin Hyung Kang[b], Young Seok Son[c]

[a] *Department of Mechanical Engineering, Yonsei University, Shinchon-Dong 134, Seodaemun-Ku, Seoul 120-749, Korea*
[b] *Department of Mechanical Engineering, Konyang University, Naldong-Ri 30, Nonsan-Eup, Nonsan-Kun, Choongnam 320-800, Korea*
[c] *Department of Mechanical Engineering, Dong-Eui University, Kaya-Dong 24, Pusanjin-Ku, Pusan 614-714, Korea*

Received 30 December 1997; in final form 10 July 1998

Abstract

Experimental investigations are made to study the double-diffusive convection phenomena of a stably-stratified salt-water solution due to lateral heating in a stationary and rotating annulus. The primary objective of this study is to obtain the basic information on the nature of natural convection with time with various parametric conditions such as rotating velocity, temperature and concentration gradients. The experiments cover the ranges of $Ar = 2.0$, $Le = 100$, $Ra_\eta = 1.57 \times 10^2$–$3.09 \times 10^5$, and $Ta = 0$–1.20×10^7. In the stationary annulus, four distinct flow regimes are observed depending on the effective Rayleigh number Ra_η: (i) stagnant flow regime, (ii) partially-formed layer flow regime, (iii) fully-formed layer flow regime, and (iv) unicell flow regime. In the rotating annulus, only fully-formed layer flow regime is observed. The temperature profile has usual inverse 'S' shape and the concentration profile is uniform in each layer due to the convective mixing both in the stationary and in the rotating cases. At the interface between adjacent layers, the temperature changes smoothly while the concentration changes rapidly. As the Taylor number (the effect of rotation) increases, the generation of rolls at the hot wall is inhibited and the formation and merging processes of layers are delayed at the given Ra_η.

Nomenclature

Ar aspect ratio, H/L
ΔC concentration difference
D diffusivity of salt
g gravitational acceleration
H height of the annulus
L width of the annulus
Le Lewis number, α/D
r radial coordinate
Ra_S solutal Rayleigh number $[g\beta_S \Delta C H^3/Dv]$
Ra_T thermal Rayleigh number $[g\beta\Delta T H^3/\alpha v]$
Ra_η effective Rayleigh number $[g\beta\Delta T\eta^3/\alpha v]$
t time
Ta Taylor number $[4\Omega^2 H^4/v^2]$
ΔT temperature difference
z axial coordinate.

Greek symbols
α thermal diffusivity
β thermal expansion coefficient
β_S solutal expansion coefficient
η reference height $[-\beta\Delta T/\beta_S(\mathrm{d}C/\mathrm{d}z)_o]$
v kinematic viscosity.
Ω angular velocity.

1. Introduction

Natural convection due to the simultaneous buoyancy forces with different diffusivities is called as double-diffusive convection. Double-diffusive convection frequently occurs in seawater flow and mantle flow in the earth's crust, as well as in many engineering applications such as solar ponds, liquid gas storages, transpiration cooling, crystal growth and metal solidification processes [1–4]. Double-diffusive convection has been a research topic of many researchers as its application fields are

* Corresponding author. Tel.: 00 822 361 2816; fax: 00 822 312 9592

0017–9310/98/$—see front matter
PII: S0017–9310(98)00226–9

expanded. As remarkable progresses in electronics and semiconductor industries require the development of crystal growth technology for high quality crystal manufacture, double diffusive convection is being studied more vigorously.

Double-diffusive convection establishes particular phenomena such as layered structures. Early works were performed for vertical temperature and concentration gradients to explain some unusual oceanographical phenomena [5]. Later investigations considered initially solute-stratified fluids that were heated or cooled from vertical enclosure walls [6–12]. The formation, interaction, and merging of convective layers were observed due to the significant difference in diffusivities of heat and mass. Recently, double diffusion induced by simultaneously imposed horizontal temperature and concentration differences has been considered [13–16]. Most recently, mechanisms responsible for high frequency oscillatory double-diffusive convection have been discussed [17–19].

In the case of lateral heating of an initially solute-stratified fluid, Chen et al. [6] suggested a characteristic length η according to the applied temperature and concentration gradients correlations. Depending on the Rayleigh number, Ra_η based on the suggested characteristic length η, two classified flow regimes such as subcritical and supercritical flow regimes were defined and studied. In the experimental and numerical studies by Lee et al. [8, 9], flow structure was divided into four distinct flow regimes depending on the buoyancy force ratios and good results were obtained for wider variable ranges. Bergman and Ungan [10] revealed the merging process of adjacent layers by flow visualization using floating material.

As mentioned previously, double-diffusive convection researches related to natural phenomena and transport phenomena of engineering applications were performed recently, but most of the existing studies were focused on flow phenomena in a stationary enclosed cavity. However, the effect of rotation often plays an important role in many transport processes such as atmospheric and oceanic flow, melting and solidification in a rotating furnace, and crystal growth by Czochralski method. In many practical engineering applications of materials processing, the entire system rotates steadily about a vertical axis. Among the researches which consider the effect of rotation, Barcilon and Pedlosky [20] observed that the effect of Ekman layer was reduced in a stably stratified fluid with the effect of rotation. A stability condition for a linear equation depending on the Taylor and Rayleigh numbers was suggested by Veronis [21] through the analytical study on the Benard convection of a rotating fluid between free boundaries. Hyun et al. [22] revealed that circumferential velocity gradient and horizontal density gradient were in balance in the core region with the effect of rotation. Lee et al. [23] investigated the double-diffusive convection phenomena due to heating from below in a rotating cylinder. Although the effect of rotation plays an important role in flow fields, most of the existing studies deal with a stationary system or single-diffusive convection in a rotating system due to either temperature or concentration gradient. Present work is motivated by such scarcity of work on double-diffusive convection in a rotating system, which should be acquired for natural phenomena and engineering applications.

In this paper, to get an understanding of the mixed effect of rotation and double-diffusion on flow fields, flow phenomena arising from lateral heating of an initially solute-stratified liquid in a stationary and rotating annulus are studied experimentally. Results are given and discussed for flow patterns and characteristics of temperature and concentration distributions with the variation of Ta and Ra_η, which is based on rotating velocity and temperature and concentration gradients, respectively. Particular attention is given to the flow regime where multi-layers are present.

2. Experimental system

The experimental apparatus consists of main and auxiliary part which provides rotation to the main part, and is shown in Fig. 1 schematically. The test section consists of a vertical transparent acrylic annulus enclosure to observe flow fields, and two reservoirs attached to the inner and outer vertical walls of the annulus to maintain constant but different temperatures at the vertical walls. Test fluid is filled in the observable annulus between the inner and outer cylinder, and each vertical wall of the annulus is maintained at constant but different temperature by circulating cold water through the inner cylinder and hot water through the outer cylinder.

The inner cylinder and test annulus are made of pyrex for flow visualization. The outer diameter of the inner cylinder is 30 mm $\times$ 1.2 mm thick and 80 mm high, and the inner diameter of the test annulus is 110 mm $\times$ 3 mm thick and 80 mm high. The top and bottom of the test section are made of 35 mm thick acrylic plate to satisfy adiabatic condition. Auxiliary experimental apparatus is composed of a driving part to provide rotation and a rotating table on which the test section, two constant temperature baths, a computer, a thermocouple feed mechanism, and an A/D converter are placed. The driving part which rotates the circular table consists of a motor, V-belt, decelerator, timing belt, and inverter. The rotating rate of the table is controlled from 3 to 60 rpm by an inverter, and a power slip ring is installed on a rotating axis to supply electrical power which is needed for the components on the table.

Initially the annulus is filled with a salt-water solution using the standard step method with 30 steps to establish the desired initial salinity profiles. It takes about two hours to have a linear concentration profile by diffusion

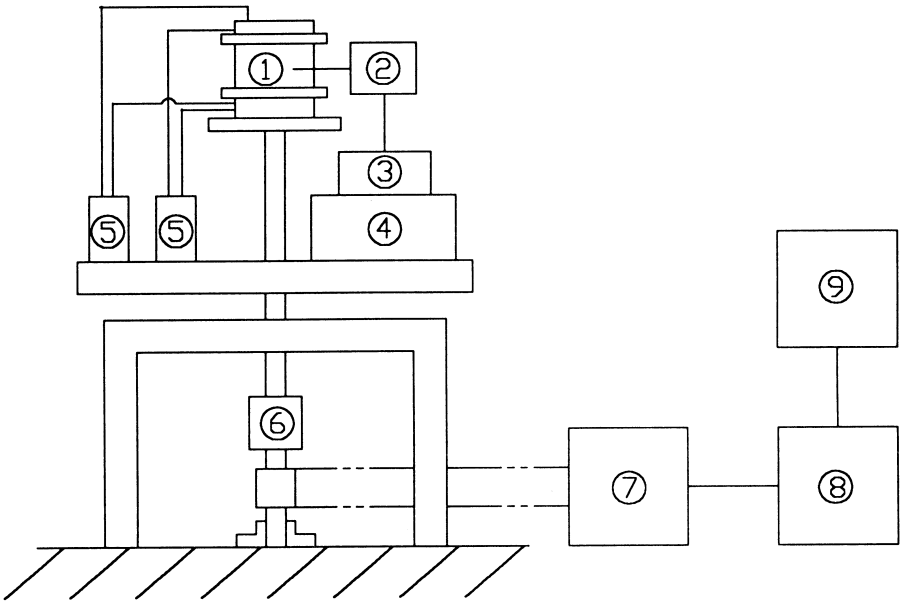

Fig. 1. View of the total experimental apparatus.

in the test section. To avoid mixing of the solution, the bottom wall is heated after the system is spun up.

To measure temperatures in the annulus, thermocouples installed at L/4, 2L/4, and 3L/4 locations are made to move vertically with a programmable stepping motor, and are connected to a 16 bit A/D converter via a pre-amplifier. This yields a resolution of 0.05°C. The thermocouples move through the solution with a speed of 20 mm/s and data are acquired at 1 kHz. Temperature distributions at 5 mm intervals are measured during rotation. The sample extraction method is used to measure concentration. A minute amount of solution is extracted through the holes which have been made at 7.3 mm intervals on the vertical wall of the annulus, and its refractive indices are read through a refractometer. This procedure is repeated several times, and the average refractive index is then converted into the concentration by a conversion chart. The deviation of the refractive indices are about $\pm 2\%$. During the initial stage of cell formation measurements of temperature and concentration are very difficult because flow pattern changes at a short time interval and the thicknesses of layers are small. Therefore, temperatures and concentrations are measured after layers are formed comparatively stably in the test annulus. A shadowgraph technique is used to observe flow fields in the annulus by flow visualization. The annulus is illuminated by passing a 10 mW He–Ne laser beam through a spatial filter assembly and the image picture is taken by a camera.

The ranges of the parameters covered in the present experiments are $\Delta T = 1.0$–11.9°C, $\Delta C = 5$–6 wt%, $\Omega = 0$–10 rpm. The corresponding nondimensional par-

ameters range as $Ra_T = 1.51 \times 10^7$–1.89×10^8, $Ra_S = 1.40 \times 10^9$–1.60×10^9, $Ra_\eta = 1.57 \times 10^2$–$3.09 \times 10^5$ and $Ta = 0$–1.20×10^7. In the results, data at three values of Ra_η are discussed. $Ra_\eta = 2.53 \times 10^2$ corresponds to $Ra_T = 3.04 \times 10^7$ ($\Delta T = 2.1^\circ$C) and $Ra_S = 1.51 \times 10^9$ ($\Delta C = 5$ wt%), $Ra_\eta = 4.14 \times 10^3$ corresponds to $Ra_T = 6.17 \times 10^7$ ($\Delta T = 4.2^\circ$C) and $Ra_S = 1.52 \times 10^9$ ($\Delta C = 5$ wt%), and $Ra_\eta = 2.01 \times 10^5$ corresponds to $Ra_T = 1.56 \times 10^8$ ($\Delta T = 12.1^\circ$C) and $Ra_S = 1.44 \times 10^9$ ($\Delta C = 5$ wt%). Also, $Ta = 3.01 \times 10^6$ and 1.20×10^7 corresponds to $\Omega = 5$ and 10 rpm, respectively.

3. Results and discussion

3.1. Stationary system

As is observed by Lee et al. [9] in the case of the rectangular cavity, four distinct flow regimes are observed depending on Ra_η in the stationary annulus; (i) stagnant flow regime, (ii) partially-formed layer flow regime, (iii) fully-formed layer flow regime, and (iv) unicell flow regime. The representative flow patterns for each flow regime are shown in Fig. 2, which are qualitatively similar to those in the rectangular cavity.

The stagnant flow regime shown in Fig. 2(a) is formed when Ra_η is small. No fluid motion occurs at all because the thermal buoyancy originated from the temperature difference at the hot wall is not enough to overcome the stable concentration stratification. Compared with the natural convection due to temperature difference only between the vertical walls, the flow should occur at a higher temperature difference due to the suppressing stable solutal stratification. Fig. 2(b) shows partially-formed layer flow regime. As temperature difference between the vertical walls increases (Ra_η increases), rolls develop near the top and bottom regions and expand to the cold wall to form a layered flow structure, while the fluid at the middle region of the enclosure still remains stagnant. As the temperature difference between the vertical walls increases more than that of the partially-formed layer flow regime, rolls generate at the upper and lower regions of the hot vertical wall initially expanding to the opposite wall. In the mean time several rolls generate successively above and below the initial rolls, which also expand to the cold wall finally forming a multicellular layered flow pattern. This layer-forming process continues until the layered flow structure fills the whole enclosure. This flow regime is called fully-formed layer flow regime and is shown in Fig. 2(c). This flow regime qualitatively agrees well with the existing works [6, 8]. When Ra_η increases much larger, thermal convection dominates and stratification due to the concentration distribution becomes negligible. In this case unicell flow regime appears as shown in Fig. 2(d), which looks like the flow pattern of natural convection due to temperature difference only.

Figure 3 shows the change of flow fields with time by flow visualization using shadowgraph technique for the representative case of $Ra_\eta = 2.01 \times 10^5$ in the fully formed layer flow regime. At $t = 10$ min. after the experiment, layers are generated successively near the upper and lower regions of the vertical wall and 13 layers are generated in the entire enclosure. As time passes, by the merging process of adjacent layers, the number of layers reduces to 5 layers at 2 h, 3 layers at 7 h, and 2 layers at 17 h. The initial thickness of layer depends on the relative strength of thermal buoyancy and solutal stratification. The lower Ra_η is, the smaller growth height of the layer is since the thermal buoyancy induced rising height of the adjacent fluid at the heated wall is small when the temperature gradient is small compared with the initial stable concentration gradient. Therefore the number of initial cells increases as Ra_η decreases. Since all the layered flow rotates in the same sense (here counterclock-wise), the upper (hotter) or lower (colder) part of each layer flow contacts with the lower (colder) or upper (hotter) part of the adjacent layer flow. Through this contact, the hotter part of each layer becomes less hot as it approaches the cold wall while the colder part of adjacent layer less cold when it approaches the hot wall. This causes the interfaces of each layer to skew slightly upwards when moving from cold wall to hot wall or vice versa.

After a layered-flow structure is formed completely, adjacent cells begin to merge with time as stated previously. The merging of adjacent layers tends to occur at the layer neighboring the comparatively thin layer in the enclosure. The merging of adjacent layers continues, and two layers are observed to exist in the enclosure after 17 h. Since the remaining two layers are thick and concentration difference between two layers is large, it would take a long time for the two layers to merge by very slow concentration diffusion. The interface between two layers moves either upwards or downwards slightly at 24 h after the experiment starts. Even though the global flow structure in the enclosure were not observed after long time (after 24 h), it is expected from the tendency of evolution of flow structure with time that unicell flow would finally exist in the enclosure. Time to reach unicell flow will be taken much longer as Ra_η decreases, because all the evolution process of flow structure proceeds much more slowly due to the reduced intensity of the thermally induced convection.

3.2. Rotating system

In this experiment, flow fields with and without rotation at the same Ra_η in fully-formed layer flow regime are observed and compared to see the effect of rotation. Figure 4 shows flow fields with time by shadowgraph technique at $Ra_\eta = 2.01 \times 10^5$ and $Ta = 3.01 \times 10^6$. When

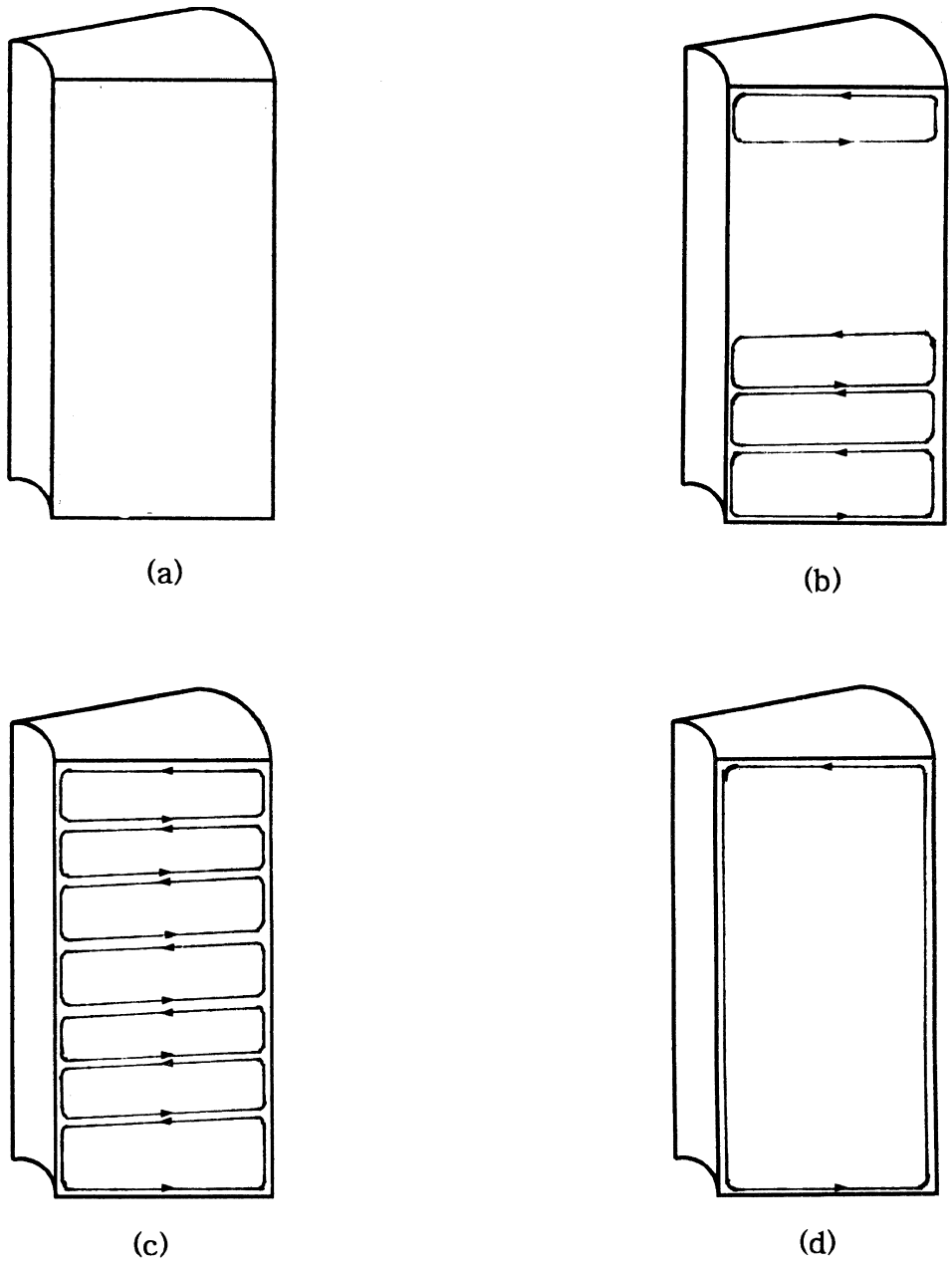

Fig. 2. Global flow patterns in the annulus for the stationary case (a) stagnant flow regime, (b) partially-formed layer flow regime, (c) fully-formed layer flow regime, (d) unicell flow regime.

flow fields are compared with those of the stationary case at the same Ra_η (Fig. 3), the mechanism of formation of rolls, developing to layered flow pattern, and merging of layers with rotation is the same as that without rotation. However, the progress of the whole process such as roll initiation and layer formation is slower due to the reduction of radial velocity by the Coriolis effect of rotation. The growth height of a roll is the same at both cases as it is determined by the ratio of thermal buoyancy to initial solutal stratification regardless of the effect of rotation, but the generation and development of rolls are suppressed due to the reduction of radial velocity by the effect of rotation.

When the number of layers with time is examined,

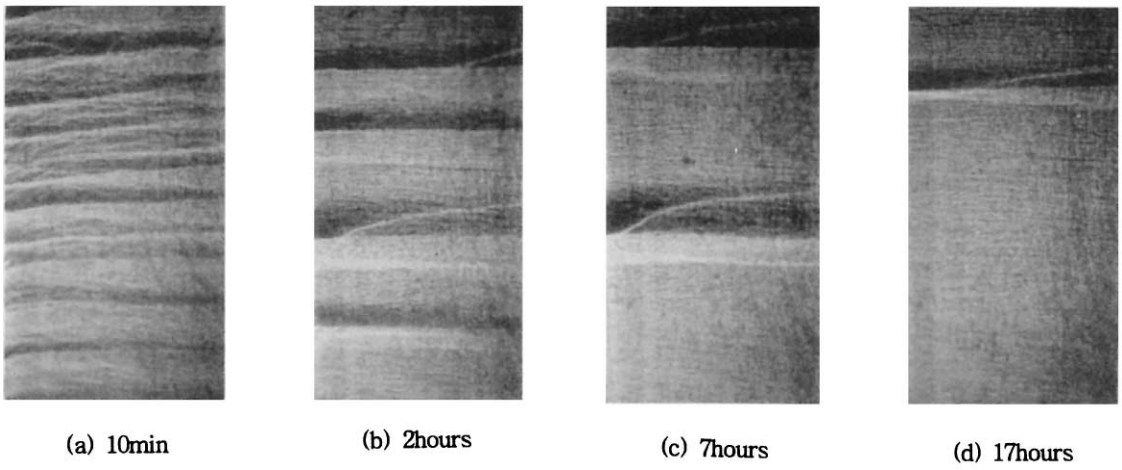

Fig. 3. Shadowgraphs of layer formation with time; $Ra_\eta = 2.01 \times 10^5$, $Ta = 0$.

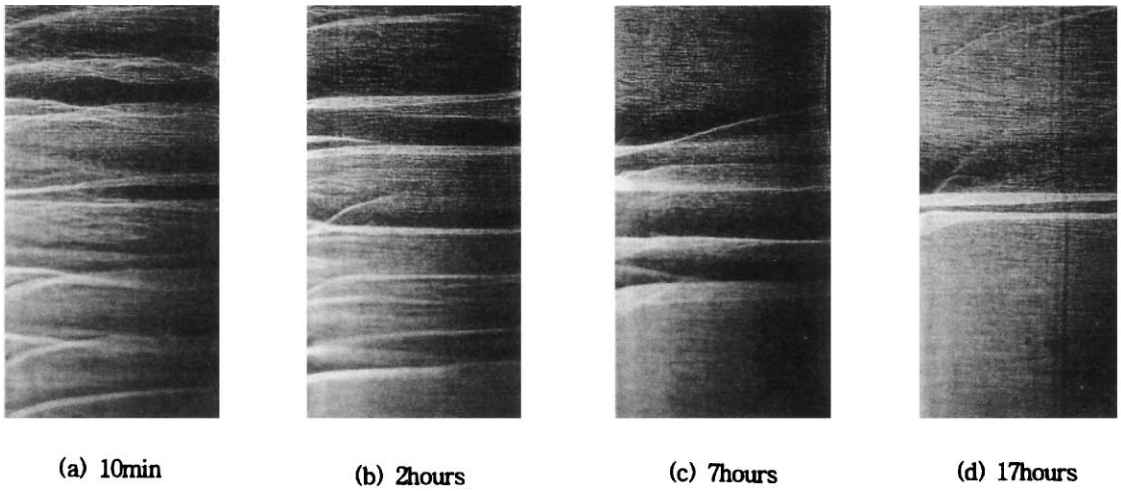

Fig. 4. Shadowgraphs of layer formation with time; $Ra_\eta = 2.01 \times 10^5$, $Ta = 3.01 \times 10^6$.

there are 8 layers at 2 h, 5 layers at 7 h, and 3 layers at 17 h in the case of $Ta = 3.01 \times 10^6$ while there are 5, 3, and 2 layers, respectively in the case of stationary system as shown in Fig. 3. This proves the delay of layered-structure formation due to the effect of rotation. Due to the reduced layer formation, the time of contact between hotter and colder layered flow is prolonged resulting in a little more inclination of interface between layers. Though it is not clear from comparison between Fig. 3 and Fig. 4, it could be seen that the interface inclines just a little bit more upwards toward hot wall in the rotation case. In addition, when Fig. 4(a) is compared with Fig. 3(a), it is established that due to suppression of layer formation by rotation, layers in the former are not formed completely at the cold wall region while layers are formed completely at about 10 min in the latter. This trend becomes more clear when the effect of rotation increases as shown in Fig. 5.

Figure 5 shows flow fields with time at $Ta = 1.20 \times 10^7$. When it is compared with Fig. 4 ($Ta = 3.01 \times 10^6$), from the number of remaining layers with time, the effect of increased rotation on the formation and evolution of layered-flow structure can be seen. Due to the increased effect of the Coriolis effect as the effect of rotation

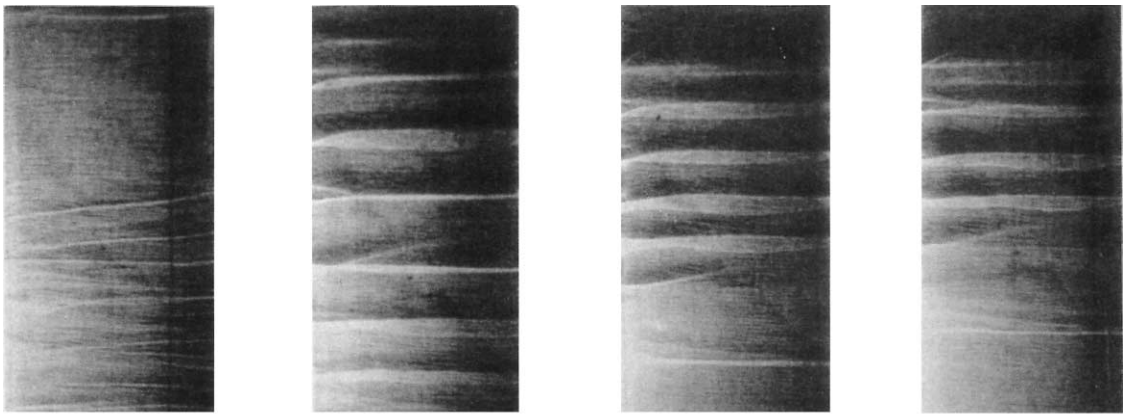

Fig. 5. Shadowgraphs of layer formation with time; $Ra_\eta = 2.01 \times 10^5$, $Ta = 1.20 \times 10^7$.

increases, the strength of flow inside each layer is more weakened and the formation and merging of layered flow structure is suppressed. At 17 h after the experiment, as mentioned previously, while the interface between cells which are merged into one moves upwards slightly in the stationary case (Fig. 3(d)), layers are on the process of merging into two from three at $Ta = 3.01 \times 10^6$ (Fig. 4(d)) and into four from five at $Ta = 1.20 \times 10^7$ (Fig. 5(d)). The interface between layers inclines a little bit more at $Ta = 1.20 \times 10^7$. When Ra_η increases at the same rotation speed, due to the increased strength of thermally driven flow at the hot wall, the number of rolls initially generated reduces and global flow evolution processes such as developing to layered flow structure and merging of layers are accelerated. It is expected that after a long time the rotating system will also have unicell flow regime due to concentration diffusion as in the stationary system.

3.3. Temperature and concentration distributions

Temperature and concentration distributions in the annulus are classified distinctly for each flow regime, and they agree well with results of the rectangular enclosure qualitatively [9]. Figure 6 shows vertical temperature and concentration profiles in the stagnant flow regime for the stationary system. Temperature profile is almost parallel to the vertical walls implying that the dominant mode of heat transfer is by conduction. Concentration profile maintains initial stably-stratified distribution. In the partially-formed layer flow regime where both stagnant flow region and layered-flow structure exist, as can be seen in Fig. 7, temperature profile shows inverse 'S' shape and concentration profile is uniform in the layered-flow region while temperature profile shows unstable distribution where the bottom temperature is higher than the top temperature and concentration profile is linear in the stagnant flow region. Almost linear unstable temperature distribution in the stagnant region results from the diffusion of heat between the cold part of the upper layered flow and the hot part of the lower layered flow across the stagnant flow region.

Figures 8 and 9 show temperature and concentration profiles with time for fully-formed layer flow regime in the stationary system and Figs 10–13 in the rotating system. Each figure shows vertical temperature and concentration profiles with time at $r/L = 0.25$, 0.5, and 0.75 in the annulus for $Ta = 0$ (without rotation), $Ta = 3.01 \times 10^6$, and $Ta = 1.20 \times 10^7$ with $Ra_\eta = 2.01 \times 10^5$. When the vertical temperature profile is observed, the temperature profile in each layer shows inverse 'S' shape like in the case of single-diffusive natural convection due to temperature difference only both in stationary and in rotating cases. Temperature changes smoothly at the interface between layers due to the relatively large thermal diffusion in contrast to the rather rapid change of concentration there. The vertical temperature profile at $r/L = 0.25$ which is nearer to the cold wall is lower than that at $r/L = 0.75$ which is close to the hot wall, and the vertical temperature profile at $r/L = 0.5$ which is at the center of the enclosure has almost the average value of both. The vertical temperature difference in each layer becomes larger in a thicker layer. From Figs 8(a), 10(a) and 12(a) horizontal temperature variation in each layer is seen to increase as the effect of rotation increases, which indicates that the conduction of heat increases relative to the effect of convection at an increased rotation.

Concentration profile in each layer is uniform due to

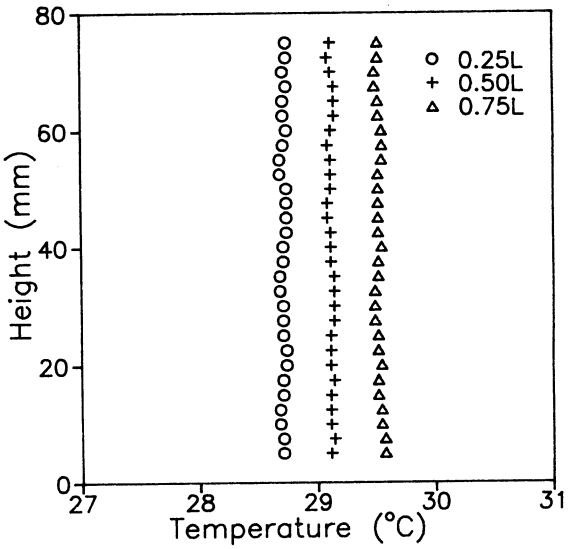

(a) Temperature profile

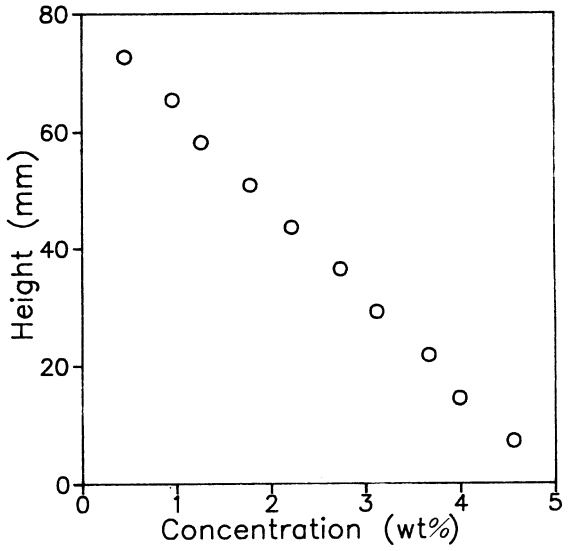

(b) Concentration profile

Fig. 6. Vertical temperature and concentration profiles at $t = 10$ h; $Ra_\eta = 2.53 \times 10^2$, $Ta = 0$ (stagnant flow regime).

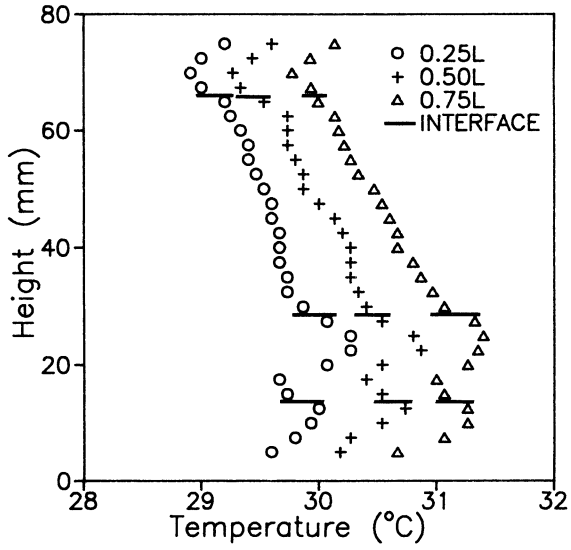

(a) Temperature profile

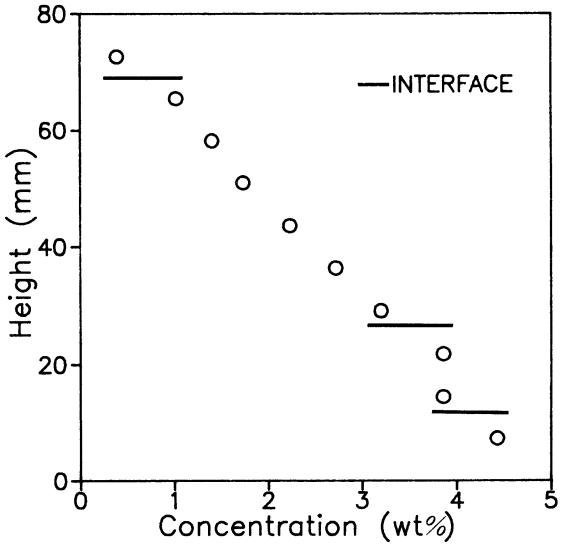

(b) Concentration profile

Fig. 7. Vertical temperature and concentration profiles at $t = 10$ h; $Ra_\eta = 4.14 \times 10^3$, $Ta = 0$ (partially-formed layer flow regime).

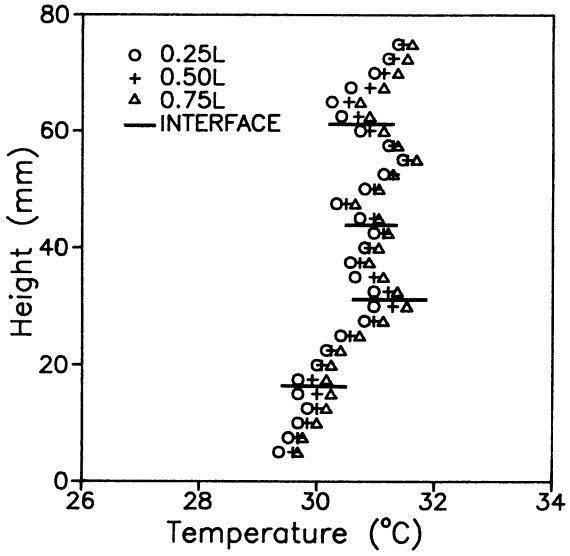

(a) Temperature profile

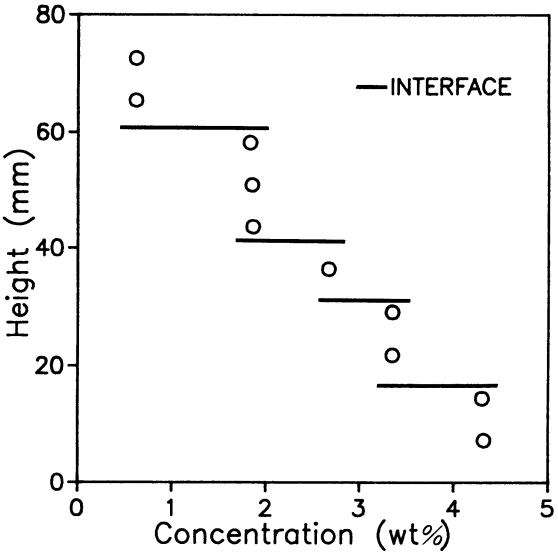

(b) Concentration profile

Fig. 8. Vertical temperature and concentration profiles at $t = 5$ h; $Ra_\eta = 2.01 \times 10^5$, $Ta = 0$ (fully-formed layer flow regime).

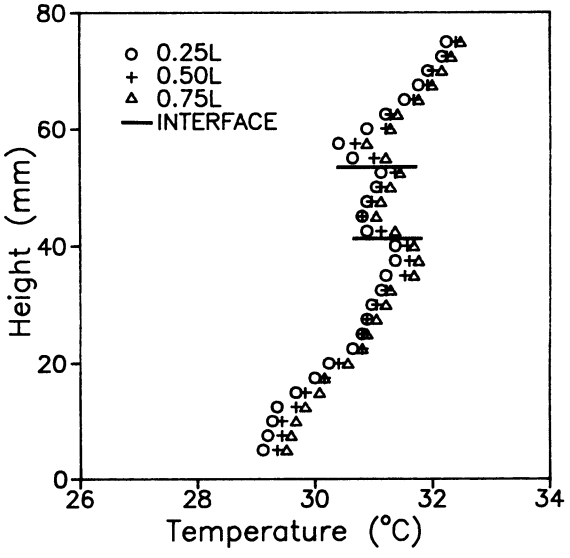

(a) Temperature profile

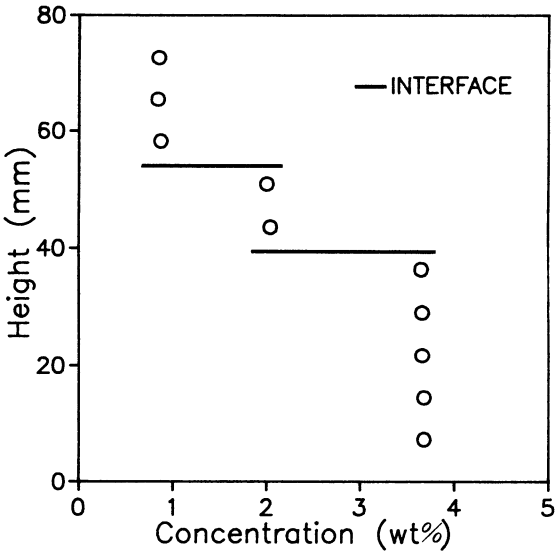

(b) Concentration profile

Fig. 9. Vertical temperature and concentration profiles at $t = 10$ h; $Ra_\eta = 2.01 \times 10^5$, $Ta = 0$ (fully-formed layer flow regime).

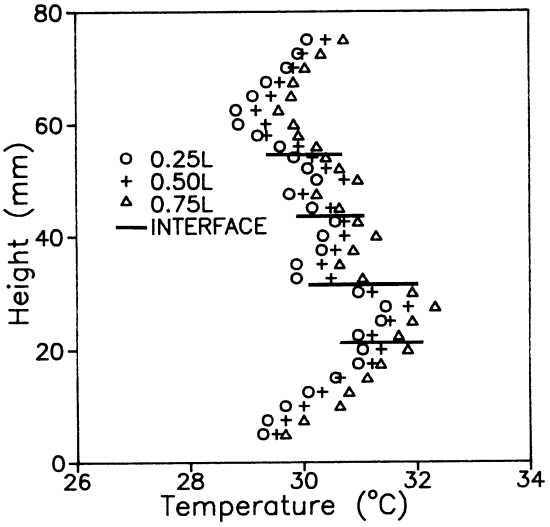

(a) Temperature profile

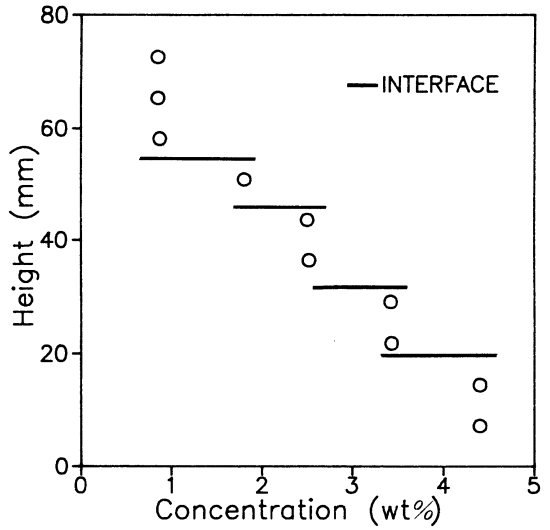

(b) Concentration profile

Fig. 10. Vertical temperature and concentration profiles at $t = 5$ h; $Ra_\eta = 2.01 \times 10^5$, $Ta = 3.01 \times 10^6$ (fully-formed layer flow regime).

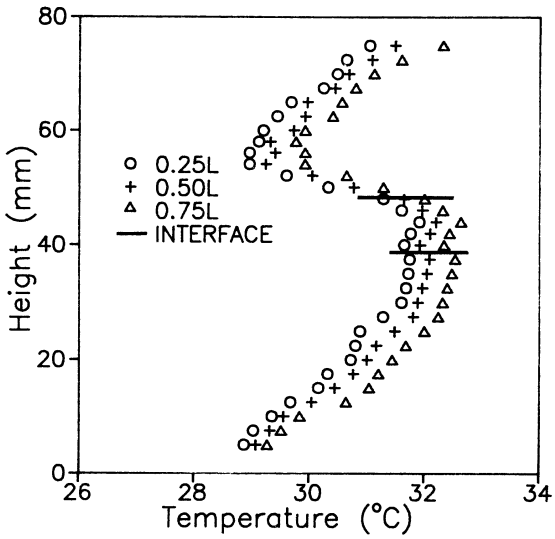

(a) Temperature profile

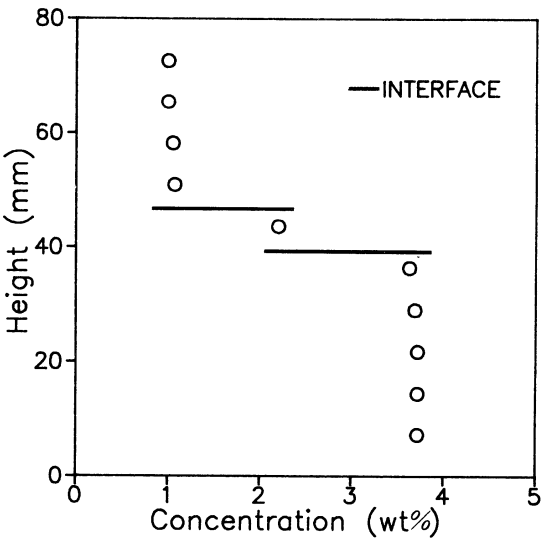

(b) Concentration profile

Fig. 11. Vertical temperature and concentration profiles at $t = 15$ h; $Ra_\eta = 2.01 \times 10^5$, $Ta = 3.01 \times 10^6$ (fully-formed layer flow regime).

the mixing by convection both in stationary and in rotating cases. As mentioned previously, since a concentration diffusion rate is much slower than a temperature diffusion rate, concentration changes rather rapidly at the interface between layers. When the number of layers decreases by merging with time, the concentration distribution in the merged layer is approximately the average of the concentration distributions of the two layers before merging.

4. Conclusions

In this paper, the double-diffusive nature of natural convection of a stably-stratified salt-water solution due to lateral heating is experimentally studied in a stationary and rotating annulus.

In the stationary annulus, four distinct flow regimes are observed depending on Ra_η and with time; stagnant flow regime, partially-formed layer flow regime, fully-

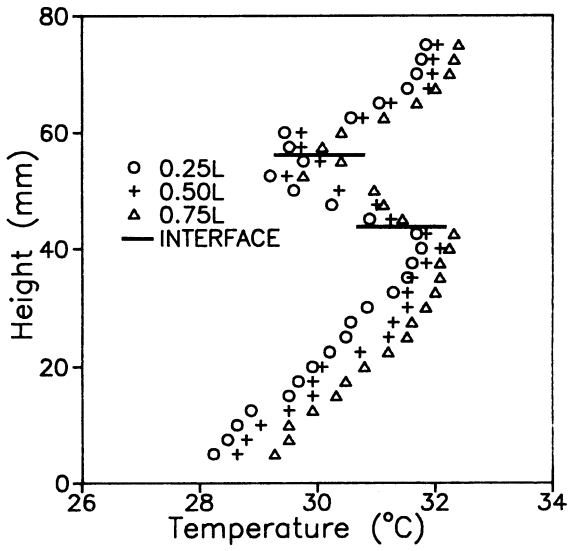

(a) Temperature profile

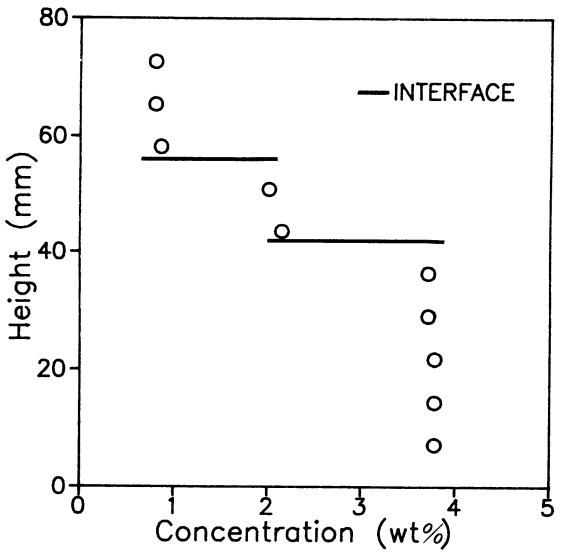

(b) Concentration profile

Fig. 12. Vertical temperature and concentration profiles at $t = 13$ h; $Ra_\eta = 2.01 \times 10^5$, $Ta = 1.20 \times 10^7$ (fully-formed layer flow regime).

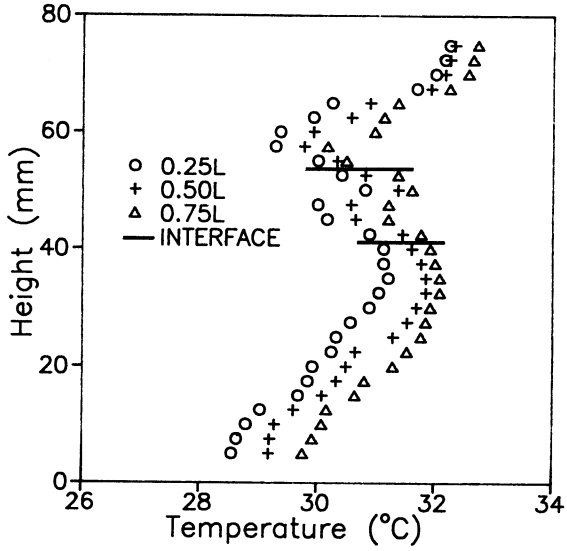

(a) Temperature profile

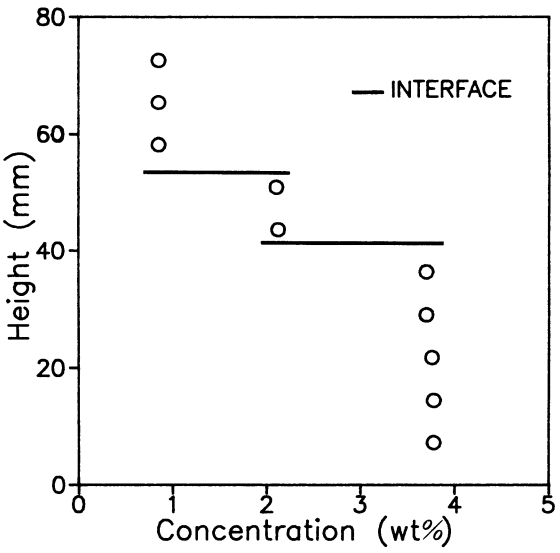

(b) Concentration profile

Fig. 13. Vertical temperature and concentration profiles at $t = 20$ h; $Ra_\eta = 2.01 \times 10^5$, $Ta = 1.20 \times 10^7$ (fully-formed layer flow regime).

formed layer flow regime, and unicell flow regime. Initial roll formation and development to layers are mainly determined by natural convection due to temperature difference, and merging of layers mainly by very slow concentration diffusion. The time to reach unicell flow regime is delayed as Ra_η decreases due to the reduced strength of the thermally-driven natural convection. Rotation effect suppresses time evolution of global flow structure such as generation of rolls at the wall, development to layers, and merging of layers, and the greater the rotation effect, the greater the suppression. The inclination of interface between layers also increases a little more according to the rotation effect. The temperature in each layer in a fully-formed layer flow regime has an inverse 'S' shape, and the concentration is uniform due to convective mixing both in stationary and in rotating

systems. The temperature changes smoothly while the concentration changes rather rapidly at the interface between adjacent layers.

References

[1] H.E. Huppert, J.S. Turner, Ice blocks melting into a salinity gradient, Journal of Fluid Mechanics 100 (1980) 367–384.

[2] R.S.J. Sparks, H.E. Huppert, J.S. Turner, The fluid dynamics of evolving magma chambers, Philosophical Transactions of the Royal Society A310 (1984) 511–534.

[3] T. Carlburg, The effect of convection upon off-eutectic composite growth of Al–Cu alloys, Journal of Crystal Growth 66 (1984) 106–120.

[4] C.F. Chen, J.S. Turner, Crystallization in a double-diffusive system, Journal of Geophysical Research 85 (1980) 2573–2593.

[5] J.S. Turner, Buoyancy Effects in Fluids, Chap. 8, Cambridge University Press, Cambridge, 1973.

[6] C.F. Chen, D.G. Briggs, R.A. Wirtz, Stability of thermal convection in a salinity gradient due to lateral heating, International Journal of Heat and Mass Transfer 14 (1971) 57–65.

[7] H.E. Huppert, R.C. Kerr, M.A. Hallworth, Heating or cooling a stable compositional gradient from the side, International Journal of Heat and Mass Transfer 27 (1984) 1395–1401.

[8] J. Lee, M.T. Hyun, J.H. Moh, Numerical experiments on natural convection in a stably stratified fluid due to sidewall heating, Numerical Heat Transfer Part A 18 (1990) 343–355.

[9] J. Lee, M.T. Hyun, Y.S. Kang, Confined natural convection due to lateral heating in a stably stratified solution, International Journal of Heat and Mass Transfer 33 (5) (1990) 869–875.

[10] T.L. Bergman, A. Ungan, A note on lateral heating in a double-diffusive system, Journal of Fluid Mechanics 194 (1988) 175–186.

[11] K. Kamakura, H. Ozoe, Numerical analysis of transient formation and degradation process of multilayered roll cells with double-diffusive natural convection in an enclosure, Numerical Heat Transfer 23 (1993) 61–77.

[12] M.T. Hyun, T.L. Bergman, Direct simulation of double-diffusive layered convection, Journal of Heat Transfer 117 (1995) 334–337.

[13] J. Lee, M.T. Hyun, Experiments on thermosolutal convection in a shallow rectangular enclosure, Experimental Thermal and Fluid Science 1 (1988) 259–265.

[14] J.M. Hyun, J.W. Lee, Double-diffusive convection in a rectangle with cooperating gradients of temperature and concentration, International Journal of Heat and Mass Transfer 33 (1990) 1605–1617.

[15] H. Han, T.H. Kuehn, Double-diffusive natural convection in a vertical rectangular enclosure—I. Experimental study, International Journal of Heat and Mass Transfer 34 (1991) 449–459.

[16] H.D. Jiang, S. Ostrach, Y. Kamotani, Unsteady thermosolutal transport phenomena due to opposed buoyancy forces in shallow enclosures, Journal of Heat Transfer 113 (1991) 135–140.

[17] C. Beckermann, C. Fan, J. Mihailovic, Numerical simulations of double-diffusive convection in a Hele–Shaw cell, Int. Video J. Engng. Res. 1 (1991) 71–82.

[18] F. Alavyoon, Y. Masuda, S. Kimura, On natural convection in vertical porous enclosures due to opposing fluxes of heat and mass prescribed at the vertical walls, International Journal of Heat and Mass Transfer 37 (1994) 195–206.

[19] M.T. Hyun, D.C. Kuo, T.L. Bergman, K.S. Ball, Direct simulation of double diffusion in low Prandtl number liquids, Numerical Heat Transfer 27 (1995) 639–650.

[20] V. Barcilon, J. Pedlosky, On the steady motions produced by a stable stratification in a rapidly rotating fluid, Journal of Fluid Mechanics 29 Part 4 (1967) 673–690.

[21] G. Veronis, Large-amplitude Benard convection in a rotating Fluid, Journal of Fluid Mechanics 31 Part 1 (1968) 113–139.

[22] J.M. Hyun, W.W. Fowlis, A. Warn-Varnas, Numerical solutions for the spin-up a stratified fluid, Journal of Fluid Mechanics 117 (1982) 71–90.

[23] J. Lee, S.H. Kang, M.T. Hyun, Double-diffusive convection in a rotating cylinder with heating from below, International Journal of Heat and Mass Transfer 40 (14) (1997) 3387–3394.